Proceedings of the ASME 2018 37th International Conference on Ocean, Offshore and Arctic Engineering
OMAE2018
June 17-22, 2018, Madrid, Spain

OMAE2018-78352

INVESTIGATING A SIMPLIFIED MODEL FOR MOONPOOL PISTON MODE RESPONSE IN IRREGULAR WAVES

Babak Ommani[*a,b]
[a]SINTEF Ocean**, Trondheim, Norway
[b]Centre for Autonomous Marine Operations and Systems (AMOS), NTNU, Trondheim, Norway
[*]babak.ommani@sintef.no

Trygve Kristiansen
Department of Marine Technology, NTNU, Trondheim, Norway

Kjetil Berget
SINTEF Ocean**, Trondheim, Norway

ABSTRACT
Estimating moonpool piston mode response at resonance is important for operation safety. This is a difficult task, in particular, due to nonlinear nature of the moonpool response connected to the damping imposed by the flow separation at the moonpool's inlet. In the present work, the applicability of a simplified model, based on decomposing the problem into potential and viscous components, is investigated. The moonpool piston mode response is modeled as an additional degree of freedom. The coupling terms between this new degree of freedom and other vessel's modes of motions are calculated based on potential flow calculations. Radiation and diffraction problems are considered separately. A finite volume solver with linearized boundary conditions is used to obtain the moonpool response under forced vertical motions. A quadratic damping model is fitted to the obtained responses and added to the free-surface condition of the potential flow formulation. The problem is solved both in frequency and time-domain. The validity of the obtained model is investigated by model test comparison for a dummy vessel with moonpool undergoing regular and irregular forced oscillations, as well as an offshore operation vessel with moonpool exposed to irregular waves. The benefits and shortcomings of the model are discussed. It is suggested that this method can be used as a practical tool to address moonpool piston mode response in irregular waves.

1 INTRODUCTION

Moonpools on offshore operation vessels provide an alternative method for installing and maintaining sub-sea modules. This is especially the case when the operation involves handling a relatively large sub-sea structure in unfavorable weather. The handling of such large sub-sea structures from offshore vessels is presently receiving attention in connection with the development of sub-sea factories [1]. In this relation, the possibility to perform all year round operation for replacement and repair is a key issue which imposes requirements on the vessel operability.

The large modules, or objects, are either handled off the side of the operating vessel, or through a moonpool. There are advantages and disadvantages in both concepts. For instance, when the object is lowered through the free-surface splash zone inside a moonpool, the object will mainly be subject to vertical hydrodynamic loads, whereas off the side of the ship, horizontal loads may be significant. To have an all year round operability, one must also consider the effects of, for instance, local breaking waves hitting the structure, which may induce local damages. On the other hand, moonpool resonance may lead to a significantly larger amplitude of the free-surface elevation in the moonpool relative to that off the side of the ship, depending on the vessel type, moonpool design and wave direction. This will affect the forces on the object not only during the splash zone phase, but also when the object is fully submerged and lowered through the moonpool, and when leaving the moonpool entrance below the ship.

Several authors have studied the moonpool resonance problem. Molin [2] presented a linearized potential flow solution to moonpool's natural modes and frequencies. Fredriksen et.al. [3] investigated forced heave combined with small forward speed or current. The effect of the current on the moonpool response was showed to be small. In [4] they investigated a moored ship section with moonpool in incoming waves. It was shown that the effect of the moonpool around the combined heave-moonpool resonance period is significant on the ship motions for their 2D case. Molin et.al. [5] investigated the gap resonance in-

**: Earlier MARINTEK, SINTEF Ocean from 1st January 2017 through a merger internally in the SINTEF Group

between two fixed, side-by-side, identical barges in irregular waves by experimental and numerical methods. They introduced mass-less plates on the surface of the gap, together with a quadratic damping term based on a fixed drag coefficient. They adopted stochastic linearization in order to properly damp the resonant response in the gap and obtain better comparison between linear frequency domain solution and experiments for the surface elevation response. More recently, Kristiansen et.al. [6] and Ommani et.al. [7] have studied the influence of object on moonpool's piston mode response.

Fast and accurate prediction of moonpool response in irregular waves is still a cumbersome challenge. Solving the problem using general purpose CFD solvers can be problematic due to the complexity of the problem and the involvement of effects with several different time-scales. This is especially true if three-hour simulations in irregular waves, and estimation of extreme responses are desired. Therefore, in the past, potential-flow based models have been proposed and used for this purpose (see for instance [5], [8] and [9]). In these studies the moonpool's free-surface vertical motion is presented as a new mode of motion for the vessel. A similar approach has been adopted in [10] where a quadratic damping model is fitted to the results of free-decay tests of moonpool's free surface.

In the present paper, the similar approach to [8] and [9] is adopted to present a simple method for modelling the piston mode response of moonpools in time-domain with irregular waves. The method is carefully validated. First the numerical results are compared against experiments for forced regular and irregular oscillations. Then, the method is validated for a freely-floating vessel with moonpool in irregular waves. The strong and weak points of the method are briefly discussed and further improvements are proposed. The moonpool nonlinear characteristics, in particular the damping due to flow separation at inlet, are identified using Potential-Viscous Coupling (PVC3D®) using forced oscillation tests. PVC3D® is a specialized in-house library developed at SINTEF Ocean as an extension to OpenFOAM® CFD package. The tool has been the center of several verification and validation studies and it is shown to be fast, robust and accurate for marine resonance problems (see for instance [6], [7] and [11]).

2 MODEL TESTS

2.1 Forced Heave

Forced heave motion experiments of a dummy ship section with moonpool were performed in the Towing Tank at SINTEF Ocean during April 2013. A photo of the model test set-up is provided in Figure 1. Irregular and regular motions were applied. Tests with empty moonpool and tests with different objects inside the moonpool were performed. In the present paper, results from the tests with empty moonpool, with regular and irregular forced heave motions are used. The results for the regular motions in presence of an object in the moonpool are previously presented and investigated in [6] and [7] by the authors.

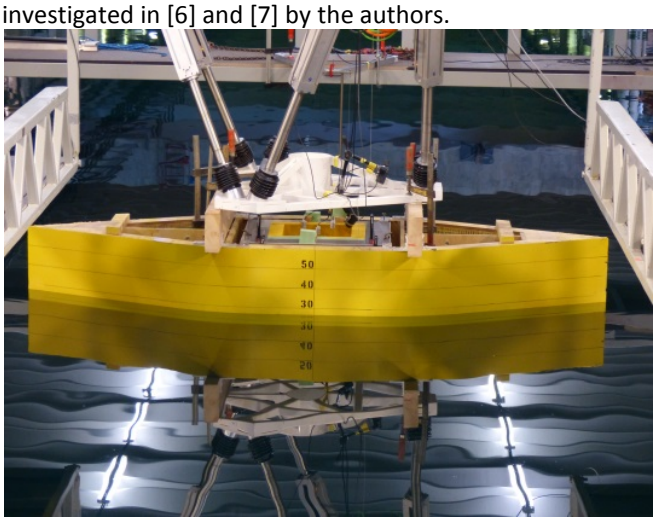

Figure 1: Photo showing the dummy ship model with moonpool mounted to the hexapod to undergo forced heave motion in the SINTEF Ocean's Towing tank.

The model scale was 1:24.5. All results given in this paper is in full scale, unless otherwise stated. The main particulars of the vessel are provided in Table 1. A sketch of the dummy ship model and main measures of the moonpool is provided in Figure 2. The 3m long model was placed transversely to the towing tank, which is 10.5m wide. Wave reflections from the side walls of the tank were reduced to an acceptably low level in this way. Parabolic beaches were used on the two far ends of the tank to absorb the radiated waves.

Table 1. Main particulars of the dummy ship used in the forced heave tests.

Parameter	Model scale	Full scale
Length	3m	73.5m
Breadth	1m	24.5m
Draft	0.249 m	6.11m
Displacement	0.497 m^3	7 238m^3
Moonpool inlet	0.294m x 0.294m	7.2m x 7.2m
Moonpool at water line	0.363m x 0.363m	8.9m x 8.9m

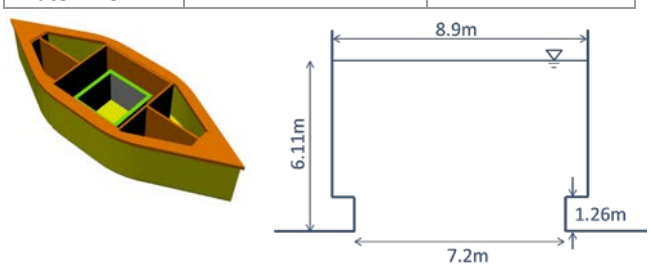

Figure 2: Left: Illustration of the dummy ship model used in the forced heave tests. Right: Full scale measures of the moonpool.

The relative moonpool elevation was recorded by means of two wave gauges placed near two of the four moonpool corners. The free-surface was observed to be nearly horizontal, i.e. dominated by the piston-mode motion. No transverse sloshing was observed during the tests. In the tests with object close to free surface, significant nonlinear effects due to the object going in and out of water were observed. These cases are investigated in [7] and are not considered in the present study.

The piston-mode time-series is taken as the averaged signal of the two wave gauges inside the moonpool. The averaged signal was band-pass filtered around the forced heave frequency *f*, with 0.9*f* as the low cut-off frequency, and 1.1*f* as the high cut-off frequency. The piston-mode amplitude was extracted from this band-pass filtered signal. The wave gauges were fixed to the model, which means that the measured free-surface elevation was that relative to the forced heave motion.

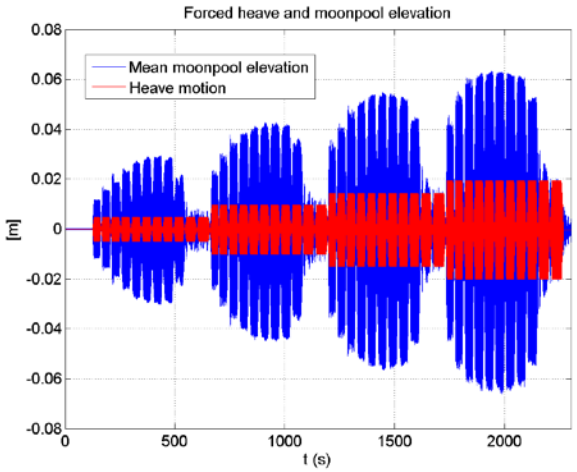

Figure 3: Time-series of heave and moonpool elevation in model scale from the regular test with empty moonpool.

The recorded time-series for the empty moonpool test with regular imposed motion is provided in Figure 3. A combination of 11 periods and 4 forcing amplitudes were performed. Thus, 44 conditions were tested in one single test. Each forcing frequency was run for 40 periods, including 5 periods of ramp-up and 5 periods of ramp-down. A time-window with duration of 10 periods, starting 12 periods after the ramp–up, was used for extracting the reduced data. The 40 period long time-series was first isolated, and band-pass filtered, then used to extract the amplitude. The forced heave motion was within 2% of what was prescribed, and with negligible amount of higher harmonics.

The same set-up is used to impose irregular motion on the dummy vessel and measure the moonpool response. The obtained signals are processed in the same way, except that the range of the band-pass filter is increased. Three different pink noise motion spectra are used (Figure 4). The motions statistics are given in Table 2. The spectrum of the obtained moonpool response for the three irregular motions are shown in Figure 5. The energy peak around 0.9[rad/s] is clear which is related to the moonpool resonance frequency. Figure 6 shows a snapshot of the imposed heave motion time series. The tests durations are 4320 seconds in full scale for each of the irregular tests.

Table 2. Statistics of forced heave motion for irregular tests

Statistics	Max	Min	Std. Dev.
Test1	0.52	-0.5	0.15
Test2	1.21	-0.95	0.3
Test3	2.2	-2.05	0.59

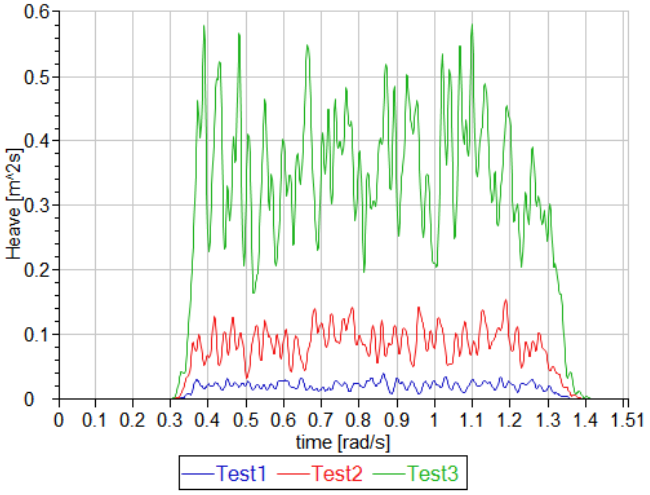

Figure 4: Forced heave motion spectrums.

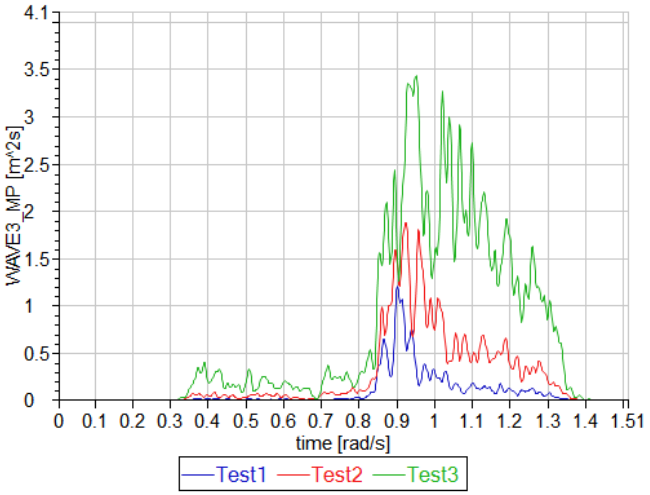

Figure 5: Recorded relative moonpool elevation for different irregular forced heave motions.

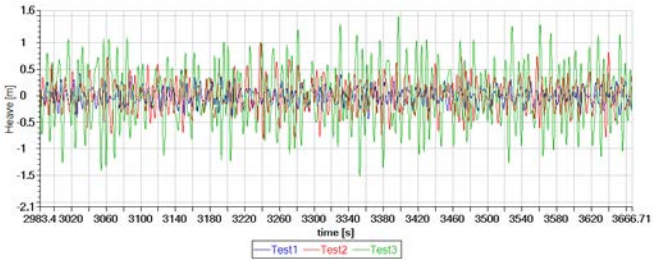

Figure 6: Snapshot of imposed irregular heave motion.

2.2 Freely-Floating Vessel in Irregular Waves

A series of model tests for an offshore operation vessel with moonpool at model scale of 1:23.17 were performed at SINTEF Ocean during summer 2016. The particulars of the vessel and its main moonpool are listed in Table 3. The vessel has three moonpools. The focus here is on the main moonpool. Due to relative size of the moonpools and vessel, it is assumed that the moonpools' response have negligible effect on the vessel's response and hence they can be studied separately. Figure 7 shows a view of the model during a test in SINTEF Ocean's basin. A horizontal mooring system has been adopted to simulate a linear restoring in horizontal modes of motion.

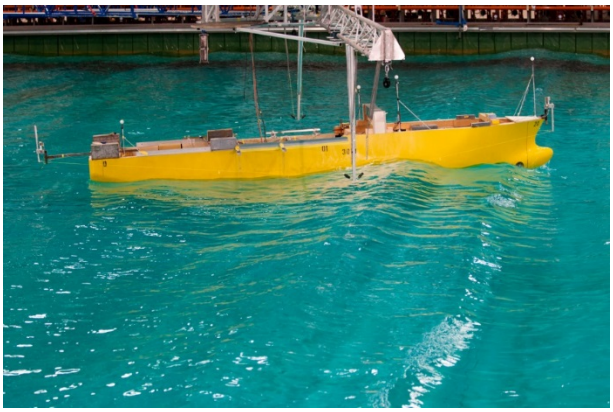

Figure 7: A view of the tested offshore operation vessel with the horizontal mooring system.

Table 3. Particulars of the tested offshore vessel, full scale.

Parameter	Unit	Value
Length between perpendiculars	(m)	138.3
Breadth	(m)	27.0
Draught, midship	(m)	6.8
Number of moonpools		3
Entrance (main moonpool)	(m)	7.2 x 7.2 x 5.2
Water Plane (main moonpool)	(m)	10.8 x 10.8

Table 4. The specifications of the selected test cases. Zero degrees wave direction corresponds to head sea.

TestNo	Hs[m]	Tp[s]	Wave Dir.[deg]
4000	3	8	0
4010	3	10	0
4200	3	8	30
4210	3	10	30

A selection of the tests from the model test program is chosen to be considered in the present study. The particulars of these tests are listed in Table 4. Free surface elevations outside the hull and inside the moonpools are measured during the tests, as well as vessel's motions in six degrees of freedom. A sketch showing the approximate location of wave probes, and the schematics of the main moonpool geometry is given in Figure 8. Two different wave headings, 0 and 30 degrees, and two different peak periods, 8 and 10 seconds, are tested for the duration of 4350 seconds full scale. The main moonpool's piston mode natural period is about 9 seconds, which falls in between the selected wave conditions.

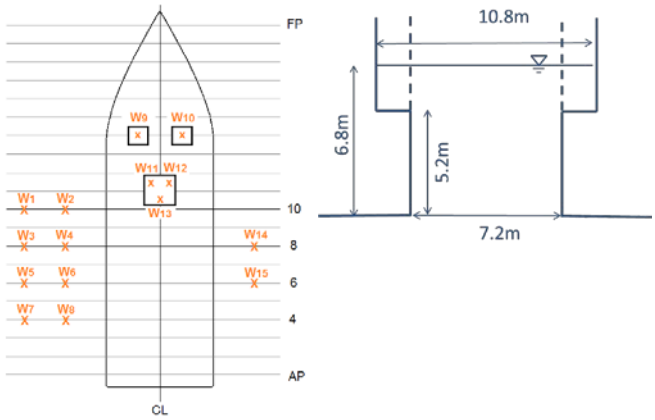

Figure 8: Sketch of the wave probes location and main moonpool geometry. W11, W12, and W13 are the three wave probes in the main moonpool.

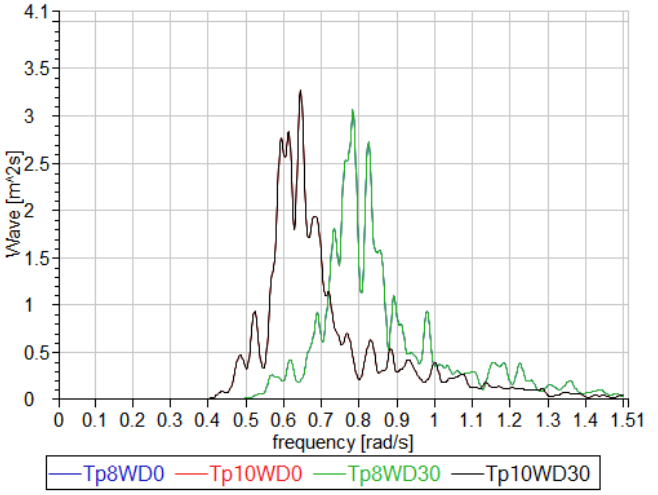

Figure 9: Comparison of incoming wave spectrums. Tp: peak period, WD: wave direction. Note that the waves with the same Tp have the same spectrum (see Table 4)

The relative elevations inside the main moonpool are recorded by three wave probes during the tests. The obtained values for all three were close and no transverse sloshing was observed, as expected for this size of moonpools. On the other hand, a clear piston mode motion was present. Figure 10 shows the vessel's heave and pitch, and main moonpool's responses during the tests. The moonpool response shows higher sensitivity to the peak period than the wave direction.

3 THEORY

A vessel with moonpool in forced motion, as well as a six-degree of freedom freely-floating vessel, are addressed in the present study. The theory is presented first for the forced motion and then generalized to be used for the floating system.

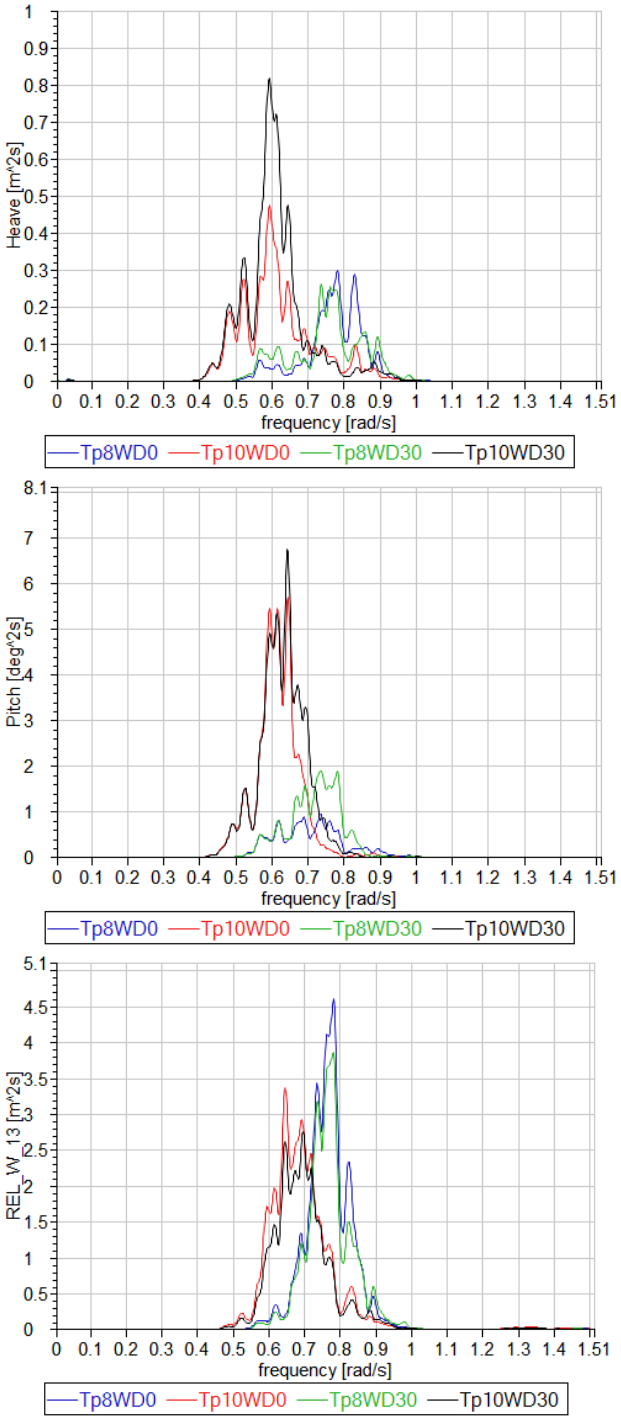

Figure 10: Responses in irregular waves for four different tests (see Table 4), Top: Vessel's heave, Middle: vessel's pitch, Bottom: Relative elevation inside the main moonpool.

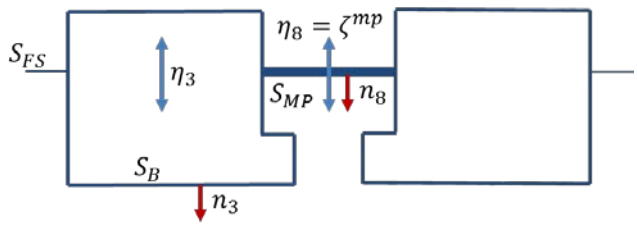

Figure 11: Schematic view of a vessel with moonpool in forced heave motions.

3.1 Forced motion in heave

A vessel with moonpool undergoing forced heave oscillations is shown in Figure 11. The linearized boundary value problem for the velocity potential Φ_3^{mp} is presented in Eqn.(1), in addition comes the radiation condition.

$$\begin{aligned} &\nabla^2\Phi_3^{mp}=0 && \text{in fluid domain} \\ &\frac{\partial\Phi_3^{mp}}{\partial n} = n_3 \qquad \dot{\eta}_3 = e^{i\omega t} && \text{on } S_B \\ &\frac{\partial\Phi_3^{mp}}{\partial n} + \frac{\omega^2}{g}\Phi_3^{MP} = 0 && \text{on } S_{FS} \text{ and } S_{MP} \end{aligned} \tag{1}$$

Here, $\Psi_3^{\mathrm{MP}}(t) = \Phi_3^{MP} e^{i\omega t}$ is assumed, and n is the unit normal vector on the surface pointing into the fluid domain. The total velocity potential for the body, with moonpool, undergoing heave motion, can be decomposed to $\Phi_3^{\mathrm{mp}} = \phi_3 + \phi_8\eta_{8_a}$. Here, ϕ_3 is the radiation potential of the body when the moonpool free-surface is replaced with a wall, for a unit amplitude of heave velocity ($\dot{\eta}_3$), and ϕ_8 is the radiation velocity potential of the moonpool free surface oscillating in piston mode (η_8). Only the vertical motion of the moonpool surface is included here, and all other modes are neglected. ϕ_8 is scaled by the resulted moonpool response, i.e. η_8. The boundary value problems for ϕ_3 and ϕ_8 are given in Eqn. (2) and (3), respectively.

$$\begin{aligned} &\nabla^2\phi_3=0 && \text{in fluid domain} \\ &\frac{\partial\phi_3}{\partial n} = 0 && \text{on } S_{MP} \\ &\frac{\partial\phi_3}{\partial n} = n_3 \qquad \dot{\eta}_3 = e^{i\omega t} && \text{on } S_B \\ &\frac{\partial\phi_3}{\partial n} + \frac{\omega^2}{g}\phi_3 = 0 && \text{on } S_{FS} \end{aligned} \tag{2}$$

$$\begin{aligned} &\nabla^2\phi_8=0 && \text{in fluid domain} \\ &\frac{\partial\phi_8}{\partial n} = 0 && \text{on } S_B \\ &\frac{\partial\phi_8}{\partial n} = n_8 \qquad \dot{\eta}_8 = e^{i\omega t} && \text{on } S_{MP} \\ &\frac{\partial\phi_8}{\partial n} + \frac{\omega^2}{g}\phi_8 = 0 && \text{on } S_{FS} \end{aligned} \tag{3}$$

Substituting $\Phi_3^{\mathrm{mp}} = \phi_3 + \phi_8\eta_{8_a}$ in Eqn. (1), and using the conditions in Eqn. (2) and (3), the Laplace equation together with body-boundary and radiation conditions are satisfied, while the free-surface boundary condition reduces to Eqn. (4),

$$\frac{\omega^2}{g}\phi_3 + \left(n_8 + \frac{\omega^2}{g}\phi_8\right)\eta_8 = 0 \qquad \text{on } S_{MP} \tag{4}$$

The coupled equations of motion for a two-degree of freedom system is given in Eqn. (5),

$$\begin{aligned} &(A_{88}\ddot{\eta}_8 + B_{88}\dot{\eta}_8 + C_{88}\eta_8) \\ &\quad +(A_{83}\ddot{\eta}_3 + B_{83}\dot{\eta}_3 + C_{83}\eta_3) = 0 \end{aligned} \tag{5}$$

Here, A_{ij}, B_{ij} and C_{ij} represent the so-called added mass, damping, and restoring coefficients in the ith mode due to motions in the jth mode (see [12] for more details). These coefficients are related to the radiation potentials as shown in Eqn. (6).

$$A_{ij} - \frac{\mathrm{i}}{\omega} B_{ij} = -\rho \iint_S n_i \phi_j dS \quad (6)$$

Here, $\mathrm{i} = \sqrt{-1}$, ρ is the fluid density, and n_i is the ith component of the normal vector on the surface S, pointing into the fluid. On the moonpool free surface (S_{MP}) we can simplify Eqn. (6) to Eqn. (7), by assuming that ϕ_j is constant on S_{MP} and $n_8 = -1$.

$$A_{8j} - \frac{\mathrm{i}}{\omega} B_{8j} = \rho \phi_j A_{MP} \qquad \text{for } j = 8,3 \quad (7)$$

Here, A_{MP} is the area of the moonpool free surface. Using Eqn. (7), assuming $\dot{\eta}_3 = e^{i\omega t}$, $\dot{\eta}_8 = \eta_{8a} e^{i\theta} e^{i\omega t}$, and setting $C_{88} = \rho g A_{MP}$ and $C_{83} = 0$, Eqn. (5) can be rearranged to,

$$(\omega^2 \phi_8 - g)\eta_8 + \omega^2 \phi_3 = 0 \quad (8)$$

The obtained relation is identical to the free-surface condition inside the moonpool in Eqn. (4). In other words, the coupled equation of motion between the body and the moonpool free-surface, ensures that the moonpool free-surface condition would be satisfied.

Similar to [5], the viscous damping due to flow separation from inlet is included in the model using a quadratic term with respect to the relative velocity between moonpool surface and body, as shown in Eqn.(9). Since it was shown that the coupled equation of motion and free-surface boundary condition are the same in this problem, this extra term will directly modify the free-surface condition by adding a kinematic damping term to Eqn. (5), such that,

$$\begin{aligned}(A_{88}\ddot{\eta}_8 + B_{88}\dot{\eta}_8 + C_{88}\eta_8) \\ +B_8^{vis}(\dot{\eta}_8 - \dot{\eta}_3)|\dot{\eta}_8 - \dot{\eta}_3| \\ +(A_{83}\ddot{\eta}_3 + B_{83}\dot{\eta}_3) = 0\end{aligned} \quad (9)$$

To solve the problem in frequency-domain, a linearized equivalent damping model is adopted. In analogy to roll damping model, the viscous damping term is replaced with $B_8^v(\dot{\eta}_8 - \dot{\eta}_3)$ where B_8^v is assumed to be a linear function of the relative amplitude, as shown in Eqn.(10).

$$B_8^v = B_8^{vL} + \frac{8}{3\pi}\omega \zeta_a^{rel} B_8^{vQ} \quad (10)$$

where $\zeta^{rel} = \zeta_a^{rel} e^{i(\omega t + \theta)} = \eta_8 - \eta_3$. The quadratic coefficient B_8^{vQ} is obtained by assuming the same averaged dissipated energy in one cycle from both models (see for instance [13] for more details). To solve the problem in time domain, memory effects needs to be considered. Therefore, Eqn.(9) is modified by including the convolution of impulse response functions (h_{ij}) as shown in Eqn.(11). More details about this time domain method could be found in [14].

$$\begin{aligned}&(A_{88}^{\infty}\ddot{\eta}_8 + C_{88}\eta_8) + B_8^{vis}(\dot{\eta}_8 - \dot{\eta}_3)|\dot{\eta}_8 - \dot{\eta}_3| \\ &+ (A_{83}^{\infty}\ddot{\eta}_3) + \int_0^t h_{88}(t-\tau)\,\dot{\eta}_8 d\tau \\ &+ \int_0^t h_{83}(t-\tau)\,\dot{\eta}_3 d\tau = 0\end{aligned} \quad (11)$$

3.2 Freely Floating Vessel in Waves

Adopting the linear decomposition of the total velocity potential, the formulation for the freely floating vessel in waves with a moonpool can be constructed in the same way. The problem is decomposed into diffraction and radiation parts. The piston mode response of the moonpool is considered as a separate mode of motion. The total velocity potential is decomposed as shown in Eqn. (12).

$$\Phi = \sum_{i-0}^{8} \phi_i \quad (12)$$

Here, ϕ_0 is the incident wave potential, $\phi_{i=1..6}$ are the radiation potentials for the six degrees of freedom, ϕ_7 is the diffracted wave potential, and ϕ_8 is the radiation potential imposed by the piston mode motion of the moonpool free-surface (see for instance [12] for more details). The coupled equation of motion between all six-degrees of freedom and moonpool motion is considered by generalizing Eqn. (11), and including the wave excitation forces, both on the vessel and moonpool surface. Any possible viscous components are neglected and only the potential wave excitation forces are included, which includes the diffracted and incident wave components.

4 NUMERICAL SIMULATIONS AND RESULTS

The equations presented in the previous section are solved using two different methods. The velocity potential functions and the wave excitation forces are obtained using WAMIT® [15]. A code is developed to solve the frequency-domain solution using the obtained radiation and excitation coefficients from WAMIT® including an equivalent linearized damping term.

The time-domain solution, using convolution integrals, is obtained using SINTEF Ocean's time-domain simulator SIMO® [16]. A new force model for the moonpool viscous damping is developed and coupled with SIMO® through a Dynamic-link Library (DLL). The simulations are performed on SINTEF Ocean's simulation platform SIMA®. Moreover, SIMA® is used for post-processing of the simulation and model test results.

An in-house finite-volume CFD library based on OpenFOAM called Potential-Viscous Coupling (PVC3D®) is used for calculating the response of the moonpool to forced heave oscillations. The results are further used to find the viscous damping coefficients. The details of the method could be found in several previous publications such as [6], [7], and [11]. The numerical setup and parameters used here are identical to the one published before in [6], and will not be repeated here.

4.1 Forced Heave Simulations and Results

The dummy vessel with moonpool, presented in Sec. 2.1 is selected for testing the present methodology. The experimental data for regular and irregular forced heave motions provide a good benchmarking case. The geometry of the vessel and the moonpool surface is modeled in WAMIT®, and the standard potential flow calculations for a

two-body system is performed. Only the heave mode of motion is included in the calculations for both bodies. The moonpool natural period is numerically identified to be 6.89[s]. A frequency-domain model is established using the obtained radiation coefficients.

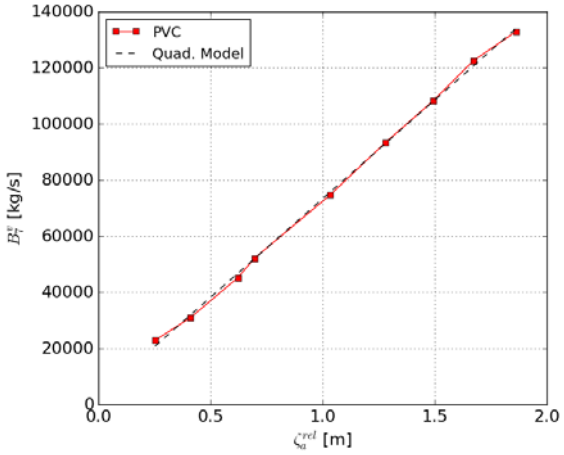

Figure 12: Equivalent moonpool damping variation with the relative moonpool amplitude for the dummy vessel at resonance period, i.e. 6.89[s]. PVC: calculations using PVC3D, Quad. Model: Fitted quadratic model.

A finite volume 3D mesh is created for the vessel with moonpool and used in PVC3D® to calculate the response of the moonpool to different regular forcing amplitudes at the resonance frequency. The dependency of the damping to oscillation frequency is neglected, and the equivalent linearized viscous damping B_8^v is obtained by fitting the model in Eqn.(9) to the obtained results. Figure 12 shows the calculated damping values and the fitted quadratic model. The dependency of the obtained damping coefficients to the relative motion amplitude seems to be well described by a quadratic model.

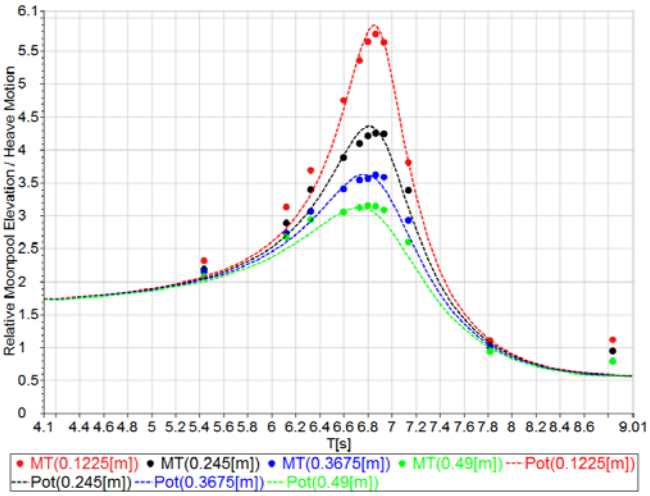

Figure 13: Non-dimensional relative moonpool response for different regular forcing amplitudes. Comparison between model test frequency-domain solution using equivalent linearized damping.

The obtained linearized damping coefficients are used together with the radiation coefficients to calculate the moonpool response in frequency-domain. Figure 13 shows the comparison between the obtained results and the model test data extracted for regular forced heave motions, and four different amplitudes. The results show acceptable agreement for regular motions. It also shows that, at a certain amplitude, a single damping coefficient can give a reasonable estimate of the response for different frequencies. The same is not true, for instance, in presence of an object in the splash zone of the moonpool [7]. The next step is to use the time-domain solver and test the model for irregular motions.

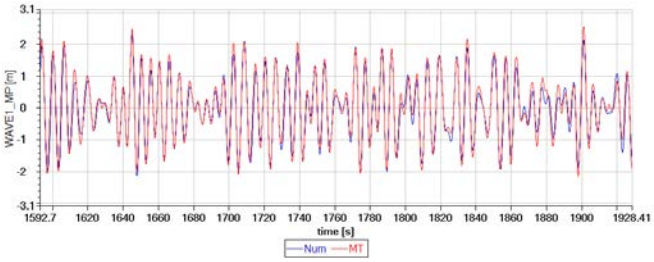

Figure 14: Time-series example for moonpool relative elevation for irregular heave motions. Num.: numerical results, MT: Model Test results

The time-domain solver is used to calculate the moonpool response for the irregular forced heave motions. The dummy vessel and moonpool are modelled in SIMO® as a two-body coupled system by introducing hydrodynamic couplings. Only heave mode of motion is included in the calculations. The recorded motion for the three tests presented in Table 2 are imposed on the vessel body, while the time-domain solver calculates the response of the moonpool. The quadratic damping model obtained from the regular motions is used here. Figure 14 shows a comparison between the obtained time series for relative moonpool elevation from simulations and model test. The simulations seem to follow the recorded elevations during model tests with satisfactory accuracy. The spectrum of moonpool elevations are compared in Figure 15, while the signals statistics are presented in Table 5. In both cases the simulation results show good agreement with the model test data.

Table 5. Statistics of moonpool response for irregular tests from model test (MT) and time domain simulation (Num)

		Max[m]	Min[m]	Std. Dev.[m]
Test1	MT	1.1	-1.21	0.36
	Num	1.06	-1	0.33
Test2	MT	1.83	-1.92	0.6
	Num	1.72	-1.8	0.56
Test3	MT	3.09	-2.66	1.01
	Num	2.92	-2.76	0.96

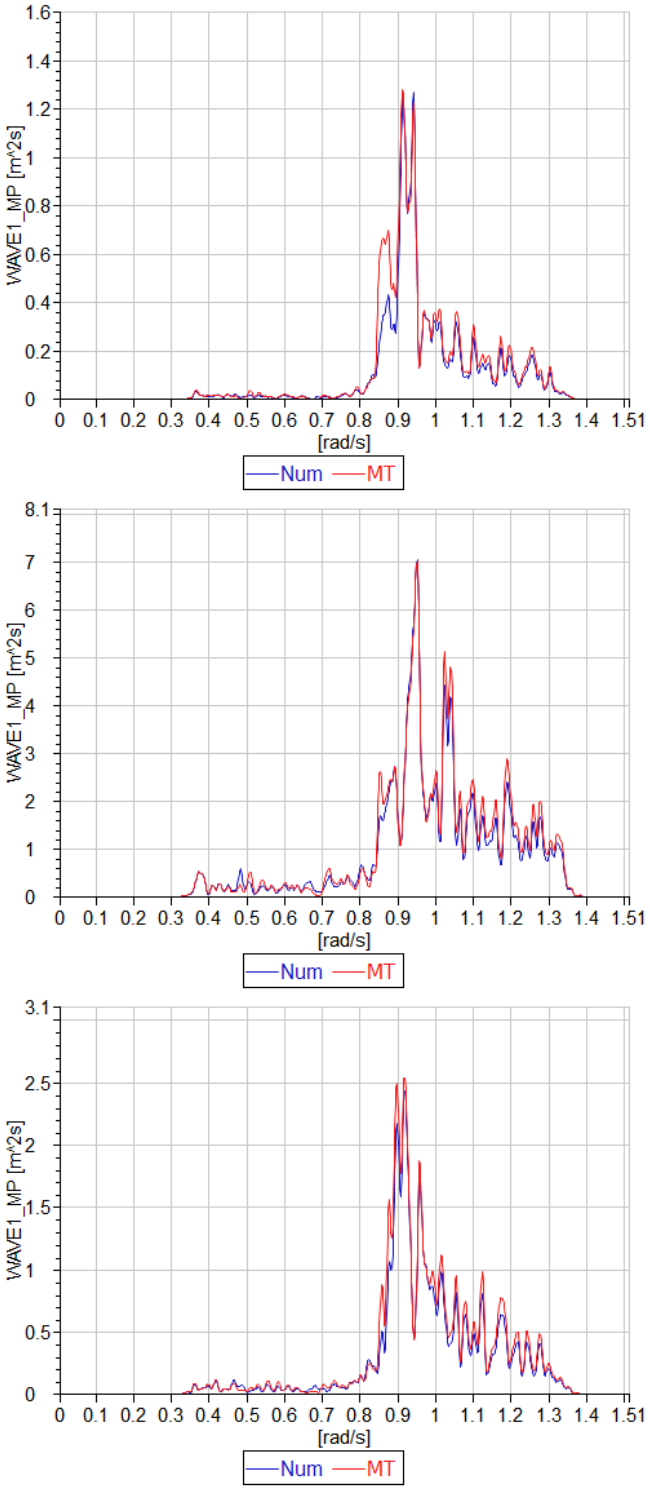

Figure 15: Moonpool relative elevation spectrums. Num: simulations, MT: Model test. Top: Test1, Middle, Test2, and Bottom: Test3, (See Table 2).

4.2 Freely-Floating Vessel in Irregular Waves

A similar procedure is applied for the freely-floating vessel presented in Sec. 2.2. The vessel and its main moonpool is modelled in WAMIT® as a coupled two-body system. The radiation and diffraction problems are solved. Only the vertical motion of moonpool, i.e. piston mode, is included in the calculations. Moreover, since the centre of the moonpool is at the middle of the ship, only the vessel's heave and pitch couplings to moonpool response is considered. The moonpool resonance period is determined numerically to be about 9 seconds.

Similar to the previous case, the relative moonpool response to regular forced oscillations at resonance frequency and different amplitudes are determined using PVC3D®. The obtained results are then used to calculate the equivalent moonpool damping coefficients by fitting the model in Eqn. (9). A quadratic model is fitted to the results and the obtained coefficients are added to the time-domain simulator model of the vessel and moonpool.

The four tests presented in Sec. 2.2 are simulated using the prepared time-domain model. It is assumed that the moonpool response has negligible influence on the vessel global response, which has been shown to hold for this type of vessel and moonpool size. In order to simplify the problem, and remove the inaccuracies in calculating the vessel's responses, the recorded heave and pitch motions during the tests, as well as incoming waves, are imposed on the vessel directly. Due to the horizontal mooring system, the vessel motions in the horizontal plane are small and neglected here. The relative moonpool elevation is calculated by considering the local heave motion of the vessel at the moonpool, i.e. $\zeta^{rel} = \eta_8 - (\eta_3 - x_{MP} \sin \eta_5)$, where x_{MP} is the longitudinal location of moonpool along the vessel, and η_5 is the vessel's pitch motion.

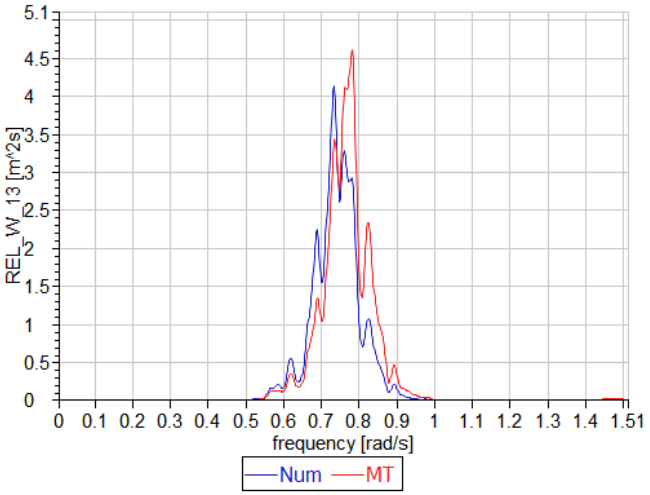

Figure 16: Relative moonpool elevation spectrum for the freely-floating vessel in irregular waves. Num: simulations, MT: model test. Test 4000 (Tp 8[s], WD 0[deg]) see Table 4. Before adjusting infinite frequency added mass in piston mode.

Figure 16 shows the comparison between the relative moonpool elevation from simulations and model test. It is possible to see that the energy in the simulation shows a shift in frequency comparing to model test. It is important to note that unlike the forced oscillation tests, the geometry of the moonpool here is complicated (see Figures 7 and 8). In particular, the change in the cross section area,

which happens close to the water line, can effectively change the added mass and restoring coefficient of the moonpool free-surface obtained for the mean water line. In other words, the system has nonlinear characteristics not only on damping, but also on added mass and restoring. A similar behaviour has been reported for moonpools with recess, which requires a separate study (see for instance [17]).

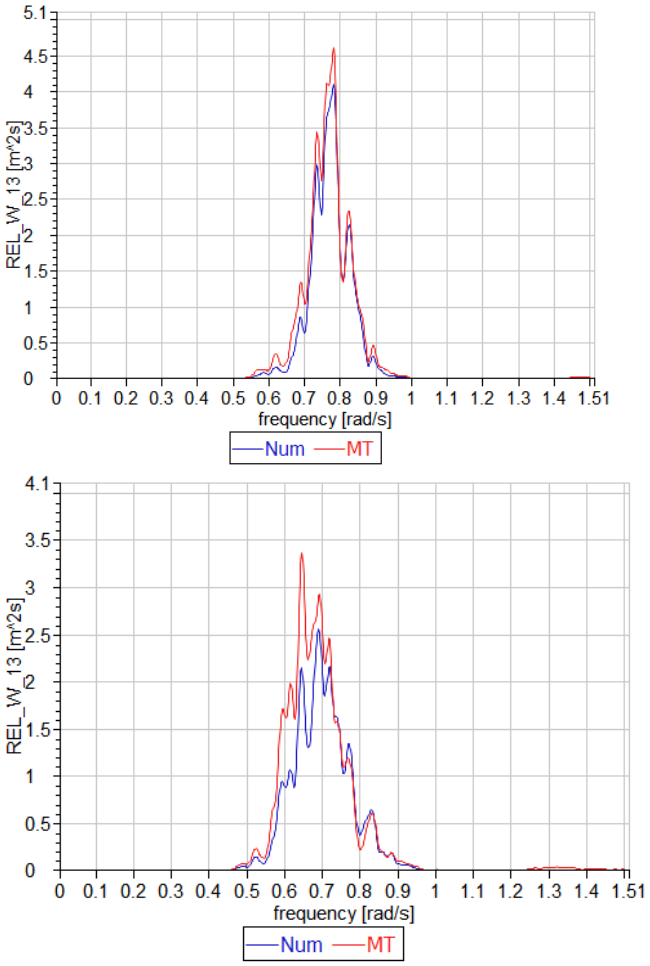

Figure 17: Relative moonpool elevation spectrum for the freely-floating vessel in irregular waves. Num: simulations, MT: model test. Top: Test 4000 (Tp 8[s], WD 0[deg]), Bot.: Test 4010 (Tp 10[s], WD 0[deg]), see Table 4.

In order to identify the limitations of the present method, the infinite frequency added mass coefficient in piston mode is decreased by 20%. This is roughly equivalent to the difference between the mass of water inside a moonpool with a constant cross section equal to the moonpool free-surface, and the present geometry. As shown in Figure 17, the adjustment corrects the shift in the spectrum to a large extent. Moreover, the distribution of energy now seems to compare reasonably well between calculations and model test. However, the accuracy of the model is not the same for different peak period and heading conditions as shown in Figure 17 and Figure 18. Looking at a time-series example can offer some explanations.

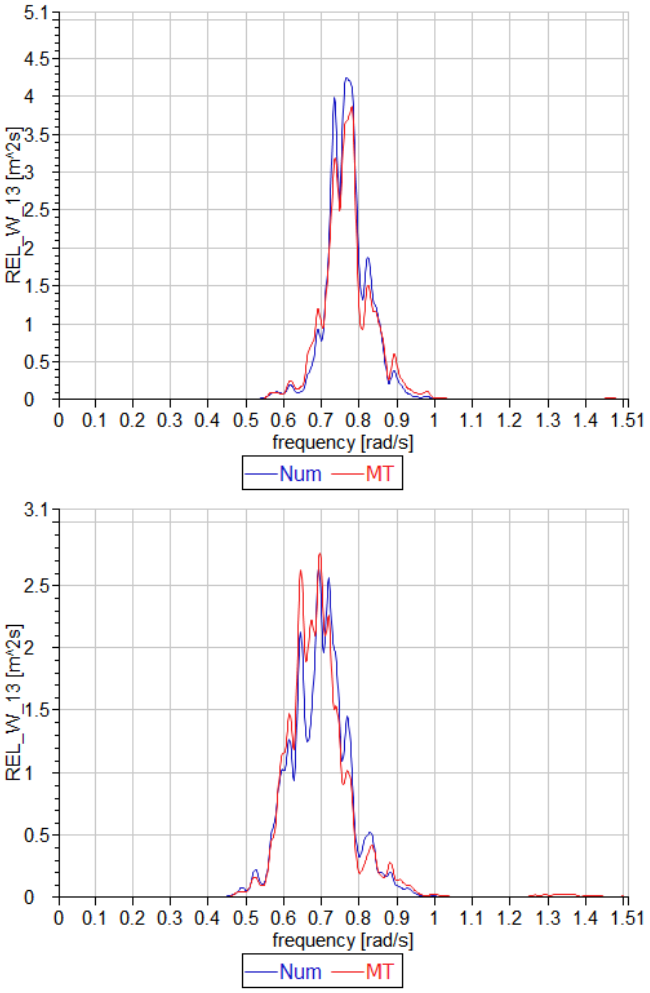

Figure 18: Relative moonpool elevation spectrum for the freely-floating vessel in irregular waves. Num: simulations, MT: model test. Top: Test 4200 (Tp 8[s], WD 30[deg]), Bot.: Test 4210 (Tp 10[s], WD 30[deg]), see Table 4.

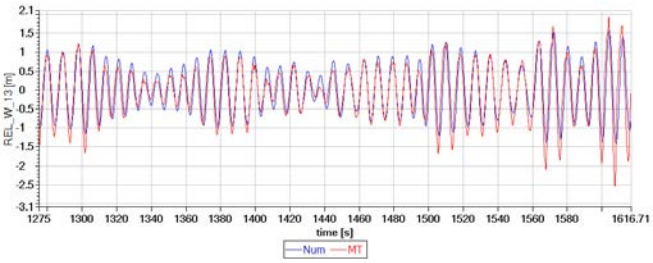

Figure 19: Time-series example for relative moonpool elevation on a freely floating vessel in irregular waves. Num: simulations, MT: model test.

Figure 19 shows a comparison between simulated and measured relative elevation inside moonpool. The general behaviour and phase of the response is well predicted. However, unlike the simple moonpool geometry used in forced oscillation tests, the positive and negative responses do not have the same magnitude. In particular, large negative responses could be identified. These appear each time the surface elevation passes the location where the moonpool cross section area changes. A smaller section means higher velocity which leads to larger responses. A more complete model is needed to address these

nonlinearities. Estimating corrections to added mass and restoring, based on location of the free-surface, using PVC3D could be one possible improvement.

5 CONCLUSIONS

In the present paper, the applicability and validity of a practical method for estimating moonpool piston mode response in irregular waves are investigated. Experimental results for moonpool response in forced motion, regular and irregular, as well as freely floating vessel in irregular waves are presented for validation. Strong nonlinearities were observed for the moonpool response in irregular waves, which were attributed to the studied moonpool geometry, in particular the change in moonpool's cross section.

The adopted mathematical model represents the moonpool free-surface as a separate single-degree-of-freedom body, and decomposes the velocity potentials. It was shown that solving the coupled equation of motion between the vessel and the moonpool free-surface leads to satisfying the free-surface boundary condition inside the moonpool. This condition is then modified by adding a quadratic damping term to account for the damping caused by flow separation at inlet. The model is implemented both in frequency and time-domain. The validity of the quadratic damping model was investigated by fitting it to the results of forced heave simulations obtained from PVC3D with success. Validating the model against forced motion model tests shown that for a clean moonpool with simple geometry the response can be estimated with good accuracy. In case of the freely-floating offshore vessel in irregular waves, the moonpool response could be predicted with reasonable accuracy. However, the observed nonlinearities, primarily due to complex moonpool geometry, could not be captured simply by a quadratic damping model. Further investigations are needed to address these nonlinearities in the model.

ACKNOWLEDGEMENTS

We acknowledge Statoil ASA for the use of forced oscillation model test data. In addition, "DSS4Lifting – Decision Support System for Crane and Lifting Operations" research project funded by the Norwegian Research Council and the project group including Salt Ship Design AS, DeepOcean AS, SINTEF Ocean AS, SINTEF Digital, Østensjø Rederi AS, UNI Research Polytec and Kongsberg Seatex, is acknowledged for the use of irregular wave model test data.

REFERENCES

[1] A. Nyhus, “Subsea technologies increase economies of marginal gas fields,” in *OTC*, Kuala Lumpur, 2014.

[2] B. Molin, “On the piston and sloshing modes in moonpools,” *J. Fluid Mech.*, vol. 430, pp. 27–50, Mar. 2001.

[3] A. G. Fredriksen, T. Kristiansen, and O. M. Faltinsen, “Experimental and numerical investigation of wave resonance in moonpools at low forward speed,” *Appl. Ocean Res.*, vol. 47, pp. 28–46, Aug. 2014.

[4] A. G. Fredriksen, T. Kristiansen, and O. M. Faltinsen, “Wave-induced response of a floating two-dimensional body with a moonpool,” *Philos. Transact. A Math. Phys. Eng. Sci.*, vol. 373, no. 2033, Jan. 2015.

[5] B. Molin, F. Remy, A. Camhi, and A. Ledoux, “Experimental and numerical study of the gap resonances in-between two rectangular barges,” in *13th congress of international maritime association of mediterranean*, Istambul, Turkey, 2009.

[6] T. Kristiansen, B. Ommani, K. Berget, and R. Baarholm, “An Experimental and Numerical Investigation of a Box-Shaped Object in Moonpool; a Three-dimensional Study,” in *Proceedings of the ASME 2015 34th International Conference on Ocean, Offshore and Arctic Engineering (OMAE2015)*, St. John’s, NL, Canada, 2015.

[7] B. Ommani, T. Kristiansen, K. Berget, P. Sandvik, and O. M. Faltinsen, “Investigation on Moonpool Blockage by Box Shaped Object Close to Free Surface,” in *3rd International Conference on Violent Flows*, Osaka, Japan, 2016.

[8] A. B. Aalbers, “The water motions in a moonpool,” *Ocean Eng.*, vol. 11, no. 6, pp. 557–579, 1984.

[9] C. H. Lee and J. N. Newman, “Computation of Wave Effects Using the Panel Method,” *WIT Trans. State--- Art Sci. Eng.*, vol. 18, p. 41, 2005.

[10] D. Chalkias and J. W. Krijger, “Moonpool behavior of a stationary vessel in waves and a method to increase operability,” in *Proceedings of the ASME 2017 36th International Conference on Ocean, Offshore and Arctic Engineering*, Trondheim, Norway, 2017.

[11] B. Ommani, T. Kristiansen, and O. M. Faltinsen, “Simplified CFD modeling for bilge keel force and hull pressure distribution on a rotating cylinder,” *Appl. Ocean Res.*, vol. 58, pp. 253–265, Jun. 2016.

[12] O. M. Faltinsen, *Sea loads on ships and offshore structures*. Cambridge, UK: Cambridge University Press, 1990.

[13] Y. Himeno, “Prediction of ship roll damping. a state of the art,” Dept. of Naval Architecture and Marine Engineering, University of Michigan, 239, 1981.

[14] W. E. Cummins, “The Impulse Response Function and Ship Motions,” David Taylor Model Basin, 1661, Oct. 1962.

[15] WAMIT, Inc., “WAMIT 7.0 User Manual.” www.wamit.com, 2013.

[16] H. Ormberg, “SIMO Theory Manual V4.0, rev 1,” MARINTEK, Trondheim Norway, MT51 F93-0184, Sep. 2012.

[17] S. Ravinthrakumar, T. Kristiansen, and B. Ommani, “A 2D Experimental and Numerical Study of Moonpools with Recess,” in *Proceedings of the ASME 2018 37th International Conference on Ocean, Offshore and Arctic Engineering*, Madrid, Spain, 2018.